substance: boron compounds with group V elements
property: properties of boron-phosphorus compounds

Boron phosphide as a new refractory semiconductor [88K1].

B_5P_3

preparation (1891M], no further information available

B_6P ($B_{12}P_2$); $B_{13}P_2$

Preparation and conditions of melt growth in [83S].

Growing of $B_{12}P_2$ crystals (transparent for visible light) from Ni solution [94Y].

Preparation of crystals from Pd and Ni flux and by chemical vapor deposition [87A2].

Preparation of $B_{12}P_2$ wafers by CVD in [94K2].

Epitaxial growth and growth conditions of $B_{12}P_2$ single crystalline films by CVD on silicon in [97K10] (see also [97K3]).

Structure, chemical bond

α-rhombohedral boron structure group

Space group: $D_{3d}^5 - R\bar{3}m$.

For structure determination, see [58P, 60W, 61L, 61M, 66S, 70E, 77M1, 77M2].

lattice parameters
(in Å)

(hexagonal presentation)

a	5.989(3)			83S
c	11.851(6)			
a	6.000(4)			86M
c	11.857(8)			
c/*a*	1.98			91L
V	369.7 Å^3			94L
a	5.95	*T* = 300 K	deficit P –10.2 %	83S
c	11.73			
a	6.11		excess P +7.9 %	
c	12.09			
a	5.9879(1)	*T* = 300 K	$^{10}B_{12}P_2$	95Y
c	11.8479(4)			
a	5.9872(3)		$^{11}B_{12}P_2$	
c	11.8470(9)			
a	5.984	*T* = 300 K	X-ray diffraction	61L,
c	11.850			61M,
				77M1,
				77M2

interatomic distances
(in Å)

d	1.74	inter-icosahedral	91L
	1.80	intra-icosahedral	
	1.66	origin to 6 B(1)	
	1.77	origin to 6 B(2)	
	2.24	X – X (chain)	
	1.91	X – 3 B(1)	

Lattice parameters in hexagonal and rhombohedral representation depending on the P/B ratio in Fig. 1 [83S].

Electronic properties

Boron phosphide as a new refractory semiconductor [88K1].

Calculated energy band structure in Fig. 2 [95L].

Electronic band structure in [84A].

Electronic band structure in [89H].

On band structure calculation, comparison with related compounds [87A1].

Calculation of the total and the partial densities of states in Fig. 3 [95L].

Density of states calculation for rhombohedral $B_{12}P_2$ and a hypothetical cubic $B_{12}P_2$ in Fig. 4 [87S1, 87S2].

Density of states calculation in [90B] and in [94B].

Density of states calculation in [86S2] (after these results $B_{12}P_2$ should be a metal in contradiction to the experimental results proving that $B_{12}P_2$ is a semiconductor).

Density of states calculation in [88W, 84A, 83A].

energy gap

calculated:

E_g	3.35	T = 300 K		83S
	2.63		Z → A(calculated)	95L
	4.75		Γ (calculated)	
	4.06		X (calculated)	
	3.10		Z (calculated)	
	2.83		A (calculated)	
	4.06		D (calculated)	
	2.5		calculated	79A

experimental:

E_g	3.46	T = 300 K	indirect-allowed	97W
	3.36		indirect-allowed	
	3.28		ind.-allowed derived from [83S]	
	3.18		indirect-allowed	
	2.75(1)	T = 300 K	indirect-allowed (Si-doped $B_{12}P_2$)	97W
	2.46(1)		indirect-allowed	
	2.17(3)		indirect-allowed	
	1.80(2)		indirect-allowed	
	1.62(3)		indirect-allowed	
	1.187(5)		deep level to parabolic band	
	0.954(3)		deep level to parabolic band	
	0.749(3)		deep level to parabolic band	
	0.569(3)		deep level to parabolic band	
	0.423(3)		deep level to parabolic band	
	0.353(3)		deep level to parabolic band	
	0.27(1)		deep level to parabolic band	
	0.175(5)		deep level to parabolic band	
	0.075(5)		deep level to parabolic band	
$E_{g,ind}$	3.3 eV	T = 300 K, $E \perp c$	optical absorption	65B, 67B

For X-ray emission, see [76D].

activation energy of the electrical conductivity

E_A	0.85 eV	$T^{-1/4}$ temperature dependence, Si-doped wafer	99K

calculated Mulliken effective charge

q	3.01(6) e	B(1)		95L
	3.13(6) e	B(2)		
	4.55(2) e	(P)		

Impurities and defects

Irradiation-induced damage rates in [95C].

Lattice properties

force field constants
(in mdyn/Å)

k_{BB}	1.556	intra-icosahedral, calculated	91B
$k_{(2-center)}$	1.75	inter-icosahedral, calculated	
$k_{icosahedron-chain}$	2.6		
$k_{chain-chain}$	2.1		

On anisotropy and effective charges in the vibration spectra of rhombohedral boron-rich solids ($B_{12}P_2$ included with transmission spectra of thin films) see [94S]. According to this paper the number of polar vibrations is larger than predicted by group theory.

IR-active one-phonon modes
(in cm^{-1})

ν/c	338	T = 300 K	from optical absorption	97W
	458			
	488			
	498		^{10}B isotope	
	608		^{11}B isotope	
	627			
	764			
	808		^{10}B isotope	
	856		^{11}B isotope	
	882			
	920			
	980		^{11}B isotope	
	1013		^{10}B isotope	

IR-active two-phonon modes
(in cm^{-1})

ν/c	1130			97W
	1169			
	1225			
	1255			
	1310			
	1354			
	1471			
	1514			
	1572			
	1624		strong	
	1680		strong	
	1740			
	1790			
	1822			
	1908		strong	
	1951			
	2025			
	2050			
	2094		probably interference peak	

acoustic phonon cutoff

	300 cm^{-1}			71S

Transport properties

electrical conductivity

σ	$10^{-3}...10^{-1}$ $\Omega^{-1}cm^{-1}$	T = 300 K	films obtained by different methods of preparation	92K, 94K1, 97K2

resistivity

ρ	$3 \cdot 10^2$ Ω cm	T = 300 K	polycrystals (temperature dependence: Fig. 5)	59G, 60G
	10^8 Ω cm	T = 300 K	epitaxial grown film	73T, 74T
	10^6 Ω cm	T = 295 K	non-colored crystals, $p = 10^{16}$ cm^{-3}	64P
	10...100 Ω cm	T = 295 K	blue-black crystals	64P

p-type conductivity [59G, 64P].

Hall mobiliy

μ_H	2.9...31.7 cm^{2}V^{-1}s^{-1}	T = 300 K	Si-doped wafer	99K

thermoelectric power

(in μV K^{-1})

S	210(20)	T = 650...850 K	probably Si-doped	92K
	800...1000	T = 400...800 K	Si-doped wafer	99K

Temperature dependence of the electric conductivity (Fig. 6a) and the thermoelectric power (Fig. 6b) of films obtained by chemical vapor deposition [92K]. n-type conduction is explained by excess P in the samples.

Temperature dependence of the electrical conductivity (Fig. 7a) and of the thermoelectric power (Fig. 7b) of CVD wafers [97K2].

Electrical conductivity and thermoelectric power of films prepared by a molecular beam deposition (MBD) process in [94K20]. According to an information by the author in a discussion at the ISBB'96, the very high thermoelectric powers (up to 10 mV/K) were erroneous.

Thermoelectric properties of boron phosphide [88K2].

Electrical and thermal properties of $B_{12}P_2$ wafers [99K].

current voltage characteristic: Fig. 8.

thermal conductivity

κ	$3.8 \cdot 10^{-1}$ W cm^{-1} K^{-1}	T = 300 K	polycrystal For temperature dependence, see Fig. 9.	71S

phonon mean free path

Λ	$2 \cdot 10^{-3}$ cm	T < 10 K		71S

Optical properties

refractive indices

n	2.64	T = 300 K	visible range	83S
n_0	2.57(15)	T = 300 K	62.2...275.8 cm^{-1}	97W
n_T	2.54(15)		2121.58...2939.35 cm^{-1}	

dielectric constants

ε_0	6.60(70)	T = 300 K	62.2...275.8 cm^{-1}	97W
ε_T	6.45(70)		2121.58...2939.35 cm^{-1}	

Note: refractive indices n_0 and n_T and the dielectric constants were obtained from interferences in optical spectra of a 40μm thick sample. The error is essentially caused by the thickness measurement with an accuracy of about ± 3μm i.e. 6%.

Calculated optical properties (optical conductivity σ_{opt}, dielectric function, energy loss function) in Fig. 10 [95L].

Absorption edge of undoped [83S] and Si-doped $B_{12}P_2$ [96W, 97W] together with luminescence spectrum [98S] in Fig. 11.

Absorption edge of amorphous $B_{13}P_2$ in Fig. 12 [91K], see also [95H].

One-phonon transmission and absorption spectra of $B_{12}P_2$ in Fig. 13 [97W].

Two-phonon spectrum of $B_{12}P_2$ in Fig. 14 [97W].

IR transmission spectrum in [76B, 87W, 94K2, 94S].

Conventionally measured and FT-Raman spectra of $B_{12}P_2$ in Fig. 15 [97W] (see also [96W]) obtained at different excitation intensities of the Nd:YAG laser. The conventionally measured Raman spectra of comparable samples [94S, 94K22] and of $^{10}B_{12}P_2$ [97A] are shown for comparison.

Raman spectra of $B_{12}P_2$ also in [86S1, 91T1].

Further properties

Debye temperature

Θ_D	1160 K		calculated from sound velocities	71S, 74G

density
(in g cm^{-3})

d	2.597	T = 300 K	X-ray	71S
	2.599(5)		pycnometric	71S
	2.594(7)		X-ray, melt grown	83S
	2.617(8)		pycnometric, melt grown	
	2.597		X-ray from liquid Ni_2P	65B
	2.589(5)		pycnometric, from liquid Ni_2P	

melting point

T_m	> 2000ºC			64P
	2120 °C		inert gas pressure 100 atm	83S

diffusion coefficient of P in B_6P

D	~$7 \cdot 10^{-11}$ cm^2s^{-1}	T = 1500 °C		89K, 94K1

bulk modulus

B_0	345 GPa	T = 300 K	semiempirical	97L

References:

1891M Moissan H.: C. R. Acad. Sci. (Paris) 113 (1891) 726.
58P Perri, J. A., La Placa, S., Post, B.: Acta Crystallogr. 11 (1958) 310.
59G Greiner, E. S., Gutowski, J. A.: J. Appl. Phys. 30 (1959) 1842.
60G Greiner, E. S.: see [60B1], p. 105.
60W Williams, F. V., Ruehrwein, R. A.: J. Am. Chem. Soc. 82 (1960) 1330.
61L La Placa, S., Post, B.: Planseeber. Pulvermetall. 9 (1961) 109.
61M Matkovich, V. I.: Acta Crystallogr. 14 (1961) 93.
64P Peret, J. L.: J. Am. Ceram. Soc. 47 (1964) 44.
65B Burmeister, R. A. Jr., Greene, P. E.: Bull. Am. Phys. Soc. Ser. 1110 (1965) 1184.
66S Sullenger, B., Kennard, Ch. L.: Sci. Am. 215 No. 7 (1966) 96.
67B Burmeister, R. A. Jr., Greene, P. E.: Trans. MS. AIME 239 (1967) 408.
70E Boron 3, T. Niemyski, ed., PWN Warsaw, 1970
70W Will, G.: see [70E], p. 119.
71S Slack, G. A., Oliver, D. W., Horn, E. H.: Phys. Rev. B 4 (1971) 1714.
73T Takigawa, M., Hirayama, M., Shohno, K.: Jpn. J. Appl. Phys. 12 (1973) 1504.
74G Golikova, O. A., Zaitsev, V. K., Orlov, V. M., Petrov, A. V., Tkalenko, F. N.: see [74G1], p. 25.
74T Takigawa, M., Hirayama, M., Shohno, K.: Jpn. J. Appl. Phys. 13 (1974) 411.
76B Becher, H.J., Thevenot, F.: Z. Anorg. Allg. Chem. 410 (1976) 274.
76D Domasbevskaya, E. P., Solovjev, N. E., Terechov, V. A., Ugai, Ya. A.: J. Less-Common Met. 47 (1976) 189.
77B Berezin, A. A., Golikova, O. A., Zaitsev, V. R., Kazanin, M. M., Orlov, V. M., Tkalenko, E. N., in:Boron and Refractory Borides, (Matkovich V. 1., ed.) Springer: Berlin, Heidelberg, New York 1977, p. 52.
77M1 Matkovich, V. I., Economy, J.: see [77B], p. 78.
77M2 Matkovich, V. I., Economy, J.: see [77B], p. 96.
79A Aleshin, V.G., Kosolapova, T.Ya., Nemoshkalenko, V.V., Serebriakova, T.I., Chudinov, M.G.: J. Less-Common Met. 67 (1979) 173.
83A Armstrong, D.R., Bolland, J., Perkins, P.G., Will, G., Kirfel, A.: Acta Crystallogr. B39 (1983) 324.
83S Slack, G.A., McNelly, T.F., Taft, E.A.: J. Phys. Chem. Solids 44 (1983) 1009.
84A Armstrong, D.R., Bolland, J., Perkins, P.G.: Theor. Chim. Acta 64 (1984) 501.
86M Morosin, B., Mullendore, A.W., Emin, D., Slack, G.A.: in: Boron-Rich Solids (AIP Conf. Proc. 140), Albuquerque, New Mexico 1985, D. Emin, T.L. Aselage, C.L. Beckel, I.A. Howard ed., American Institute of Physics: New York, 1986, p. 70.
86S1 Shelnutt, J.A., Morosin, B., Emin, D., Mullendore, A., Slack, G.A., Wood, C.: in: Boron-Rich Solids (AIP Conf. Proc. 140), Albuquerque, New Mexico 1985, D. Emin, T.L. Aselage, C.L. Beckel, I.A. Howard ed., American Institute of Physics: New York, 1986, p. 312.
86S2 Switendick, A.C.: in: Boron-Rich Solids (AIP Conf. Proc. 140), Albuquerque, New Mexico 1985, D. Emin, T.L. Aselage, C.L. Beckel, I.A. Howard ed., American Institute of Physics: New York, 1986, p. 260.
87A1 Armstrong, D.R.: in: Proc. 9th Int. Symp. Boron, Borides and Rel. Compounds, University of Duisburg, Germany, Sept. 21 - 25, 1987, H. Werheit ed., University of Duisburg: Duisburg, 1987, p. 125.
87A2 Aselage, T.L.: in: Novel Refractory Semiconductors, MRS Symp. Proc. Vol. 97, D. Emin, T.L. Aselage, C. Wood ed., Materials Research Soc.: Pittsburgh, 1987, p. 101.
87S1 Switendick, A.C.: in: Novel Refractory Semiconductors, MRS Symp. Proc. Vol. 97, D. Emin, T.L. Aselage, C. Wood ed., Materials Research Soc.: Pittsburgh, 1987, p. 45.
87S2 Switendick, A.C.: in: Proc. 9th Int. Symp. Boron, Borides and Rel. Compounds, University of Duisburg, Germany, Sept. 21 - 25, 1987, H. Werheit ed., University of Duisburg: Duisburg, 1987, p. 349.
87W Werheit, H., Haupt, H.: Z. Naturforsch. 42a (1987) 925.
88K1 Kumashiro, Y.: New Mater. New Processes 4 (1988) 1.
88K2 Kumashiro, Y., Hirabayashi, M., Koshiro, T., Okada, Y.: J. Less-Common Met. 143 (1988) 159.
88W Werheit, H., Kuhlmann, U., Tanaka, T.: (unpublished results).
89H Hatakeyama, T.: in: Electronic Structures of Icosahedral Boron Solids, University of Tokyo ed., Tokyo, 1989.
89K Kovalev, A.V., Tkachenko, V.F., Taran, A.A., Paderno, Yu.B., Paderno, V.N.: Neorg. Mater. 25 (1989) 968.
90B Bullett, D.W.: in: The Physics and Chemistry of Carbides, Nitrides and Borides; NATO ASI Series E: Applied Sciences Vol. 185, R. Freer ed., Kluwer Academic Publishers: Dordrecht, 1990, p. 513.

91B Beckel, C.L., Yousaf, M.: in: Boron-Rich Solids, Proc. 10th Int. Symp. Boron, Borides and Rel. Compounds, Albuquerque, NM 1990 (AIP Conf. Proc. 231), D. Emin, T.L. Aselage, A.C. Switendick, B. Morosin, C.L. Beckel ed., American Institute of Physics: New York, 1991, p. 312.

91K Kimura, K.: J. Non-Cryst. Solids 137&138 (1991) 919.

91L Lundström, T.: in: Boron-Rich Solids, Proc. 10th Int. Symp. Boron, Borides and Rel. Compounds, Albuquerque, NM 1990 (AIP Conf. Proc. 231), D. Emin, T.L. Aselage, A.C. Switendick, B. Morosin, C.L. Beckel ed., American Institute of Physics: New York, 1991, p. 186.

91T1 Tallant, D.R., Aselage, T.L., Emin, D.: in: Boron-Rich Solids, Proc. 10th Int. Symp. Boron, Borides and Rel. Compounds, Albuquerque, NM 1990 (AIP Conf. Proc. 231), D. Emin, T.L. Aselage, A.C. Switendick, B. Morosin, C.L. Beckel ed., American Institute of Physics: New York, 1991, p. 301.

91T2 Tushishvili, M.Ch., Darsavelidze, G.Sh., Tsagareishvili, O.A., Bairamashvili, I.A., Jobava, J.Sh.: in: Boron-Rich Solids, Proc. 10th Int. Symp. Boron, Borides and Rel. Compounds, Albuquerque, NM 1990 (AIP Conf. Proc. 231), D. Emin, T.L. Aselage, A.C. Switendick, B. Morosin, C.L. Beckel ed., American Institute of Physics: New York, 1991, p. 582.

92K Kumashiro, Y., Yokoyama, T., Nakamura, J., Matsuda, K., Yoshida, H., Takahashi, J.: in: Mater. Res. Soc. Symp. Proc. Vol. 242, Mater. Res. Soc. 1992, p. 629.

94B Bullett, D.W.: Proc. 11th Int. Symp. Boron, Borides and Rel. Compounds, Tsukuba, Japan, August 22 - 26, 1993, Jpn. J. Appl. Phys. Series 10 (1994), p. 31.

94K1 Kumashiro, Y., Yokoyama, T., Nakamura, J., Takahashi, J.: Proc. 11th Int. Symp. Boron, Borides and Rel. Compounds, Tsukuba, Japan, August 22 - 26, 1993, Jpn. J. Appl. Phys. Series 10 (1994), p. 168.

94K2 Kumashiro, Y., Yoshizawa, H., Shirai, K.: Proc. 11th Int. Symp. Boron, Borides and Rel. Compounds, Tsukuba, Japan, August 22 - 26, 1993, Jpn. J. Appl. Phys. Series 10 (1994), p. 166.

94L Lundström, T., Bolmgren, H.: Proc. 11th Int. Symp. Boron, Borides and Rel. Compounds, Tsukuba, Japan, August 22 - 26, 1993, Jpn. J. Appl. Phys. Series 10 (1994), p. 1.

94S Shirai, K., Gonda, S., Kumashiro, Y.: Proc. 11th Int. Symp. Boron, Borides and Rel. Compounds, Tsukuba, Japan, August 22 - 26, 1993, Jpn. J. Appl. Phys. Series 10 (1994), p. 102.

94Y Yang, P., Aselage, T.L.: Proc. 11th Int. Symp. Boron, Borides and Rel. Compounds, Tsukuba, Japan, August 22 - 26, 1993, Jpn. J. Appl. Phys. Series 10 (1994), p. 130.

95C Carrard, M., Emin, D., Zuppiroli, L.: Phys. Rev. B 51 (1995) 11270.

95H Hori, A., Takeda, M., Yamashita, H., Kimura, K.: J. Phys. Soc. Jpn. 64 (1995) 3496.

95L Li, Dong, Ching, W.Y.: Phys. Rev . B 52 (1995) 17073.

95Y Yang, P., Aselage, T.L.: Powder Diffr. 10 (1995) 263.

96W Werheit, H., Kuhlmann, U., Shirai, K., Kumashiro, Y.: J. Alloys Compounds 233 (1996) 121.

97A Aselage, T., Tallant, D.R., Emin, D.: Phys. Rev. B 56 (1997) 3122.

97K1 Kumashiro, Y., Yoshizawa, H., Tokoyama, T.: J. Solid State Chem. 133 (1997) 104 (Proc. 12th Int. Symp. Boron, Borides and Rel. Compounds, Baden, Austria, 1996).

97K2 Kumashiro, Y., Yokoyama, T., Sato, A., Ando, Y.: J. Solid State Chem. 133 (1997) 314 (Proc. 12th Int. Symp. Boron, Borides and Rel. Compounds, Baden, Austria, 1996).

97K3 Kumashiro, Y., Yokoyama, T., Sakamoto, T., Fujita, T.: J. Solid State Chem. 133 (1997) 269 (Proc. 12th Int. Symp. Boron, Borides and Rel. Compounds, Baden, Austria, 1996).

97L Lee, S.P., Kim, C.K., Nahm, K., Mittag, M., Jeong, Y.H., Ryu, C.M.: J. Appl. Phys. 81 (1997) 2454.

97W Werheit, H., Kuhlmann U., Shirai, K., Kumashiro, Y.: J. Solid State Chem. 133 (1997) 140 (Proc. 12th Int. Symp. Boron, Borides and Rel. Compounds, Baden, Austria, 1996).

98S Schmechel, R.: Thesis, Gerhard-Mercator University Duisburg, Germany, 1998.

99K Kumashiro, Y., Yokoyama, T., Ando, Y.: J. Solid State Chem. (2000) (Proc. 13th Int. Symp. Boron, Borides and Rel. Compounds, Dinard, France, Sept. 1999).

99W Werheit, H., Schmechel, R., Kuhlmann, U., Kampen, T.U., Mönch, W., Rau, A.: J. Alloys Compounds 291 (1999) 28.

Fig. 1.

$B_{12}P_2$. Unit cell parameters vs. P/B ratio. **(a)** hexagonal and **(b)** rhombohedral representation [83S].

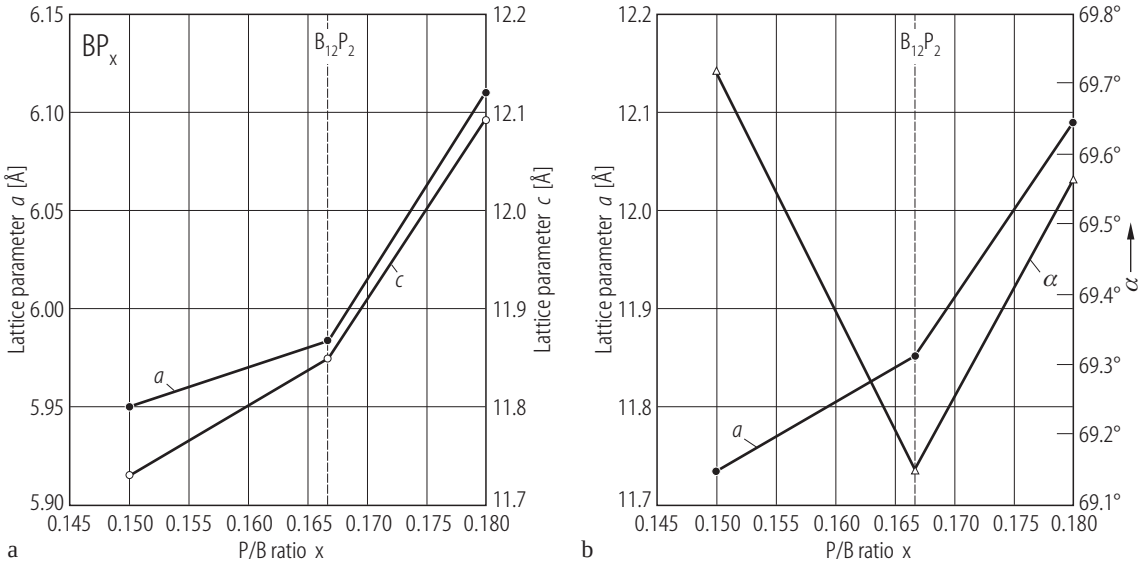

Fig. 2.

$B_{12}P_2$. Electronic band structure, calculated with the first-principles orthogonalized linear combination of atomic orbitals method [95L].

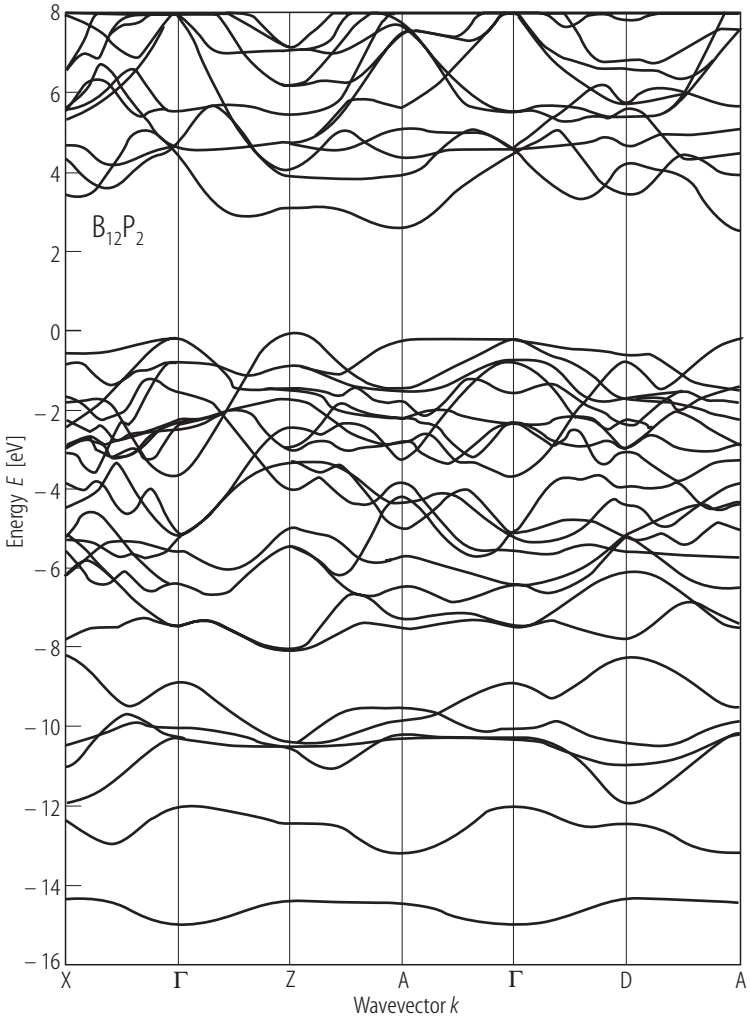

Fig. 3.

$B_{12}P_2$. **(a)** Total density of states, **(b)** partial density of states for B and **(c)** partial density of states for P vs. energy [95L].

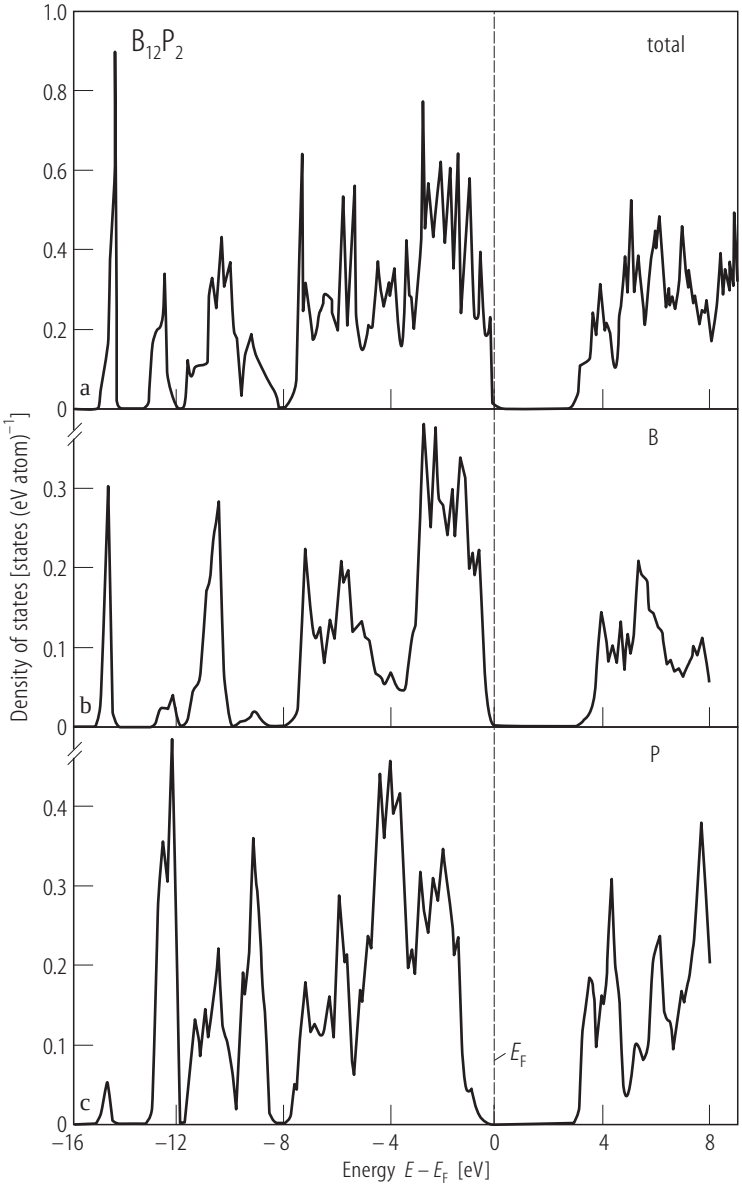

Fig. 4.

$B_{12}P_2$. Calculated density of states vs. energy, **(a)** for a hypothetical cubic $B_{12}P_2$ and **(b)** the rhombohedral $B_{12}P_2$ [87S1, 87S2].

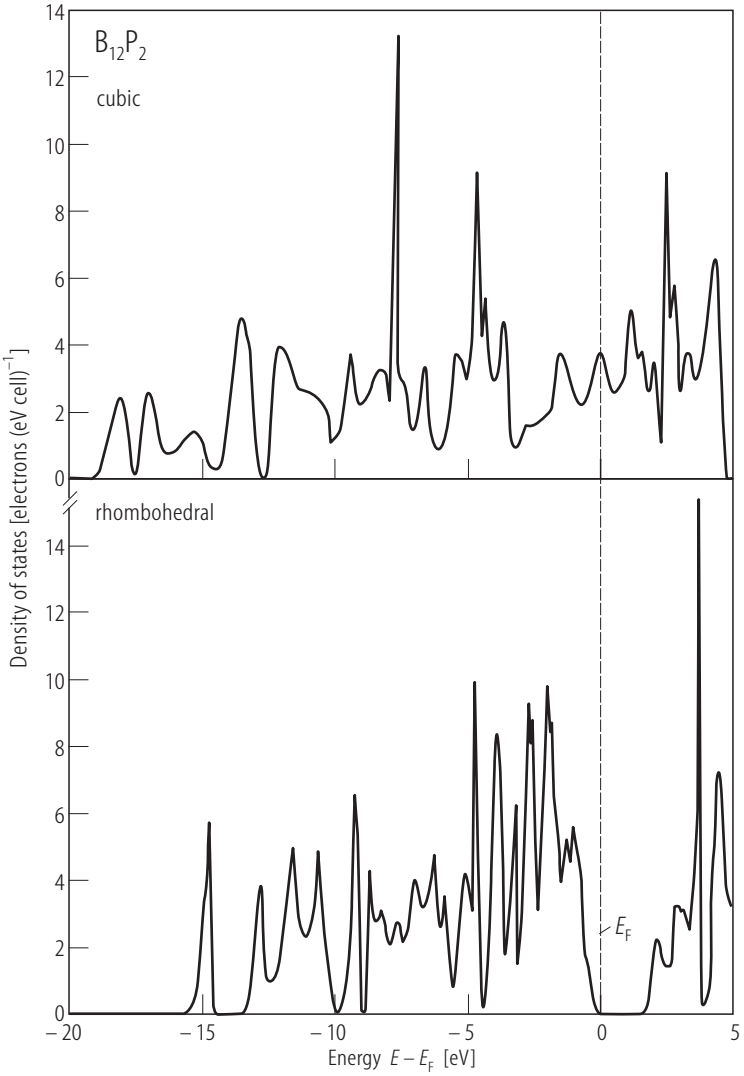

Fig. 5.

B_6P ($B_{5.8}P$). Electrical resistivity vs. reciprocal temperature for two polycrystalline samples with a phosphorus content of 14.7 at% [59G].

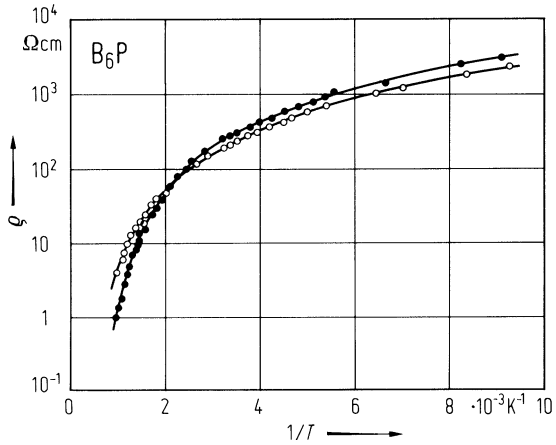

Fig. 6.

$B_{12}P_2$ (CVD). Temperature dependence of **(a)** electrical conductivity and **(b)** thermoelectric power. Substrate temperatures T_s = 800 °C; 900 °C; 1000 °C; full circles: "$B_{13}P_2$" (information on the condition of preparation is missing) [92K].

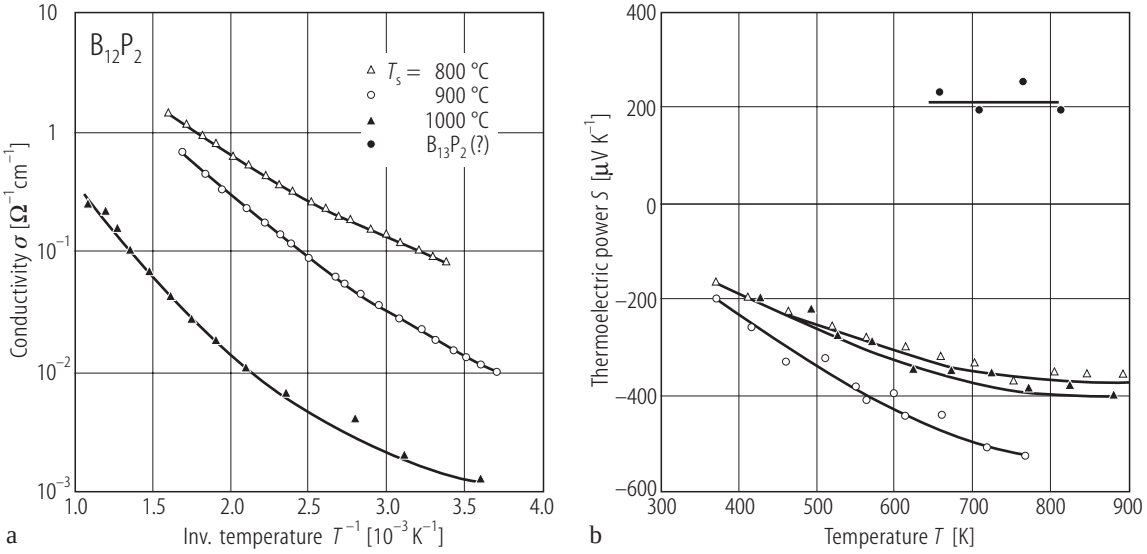

Fig. 7.

$B_{12}P_2$ (wafer). Temperature dependence of **(a)** electrical conductivity and **(b)** thermoelectric power [97K2].

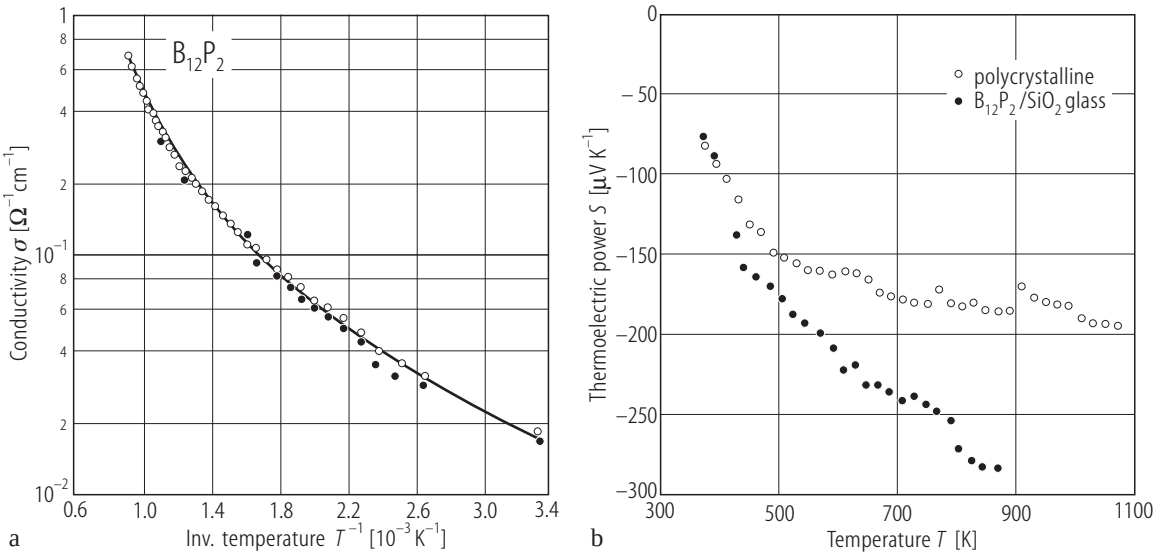

Fig. 8.

$B_{13}P_2$. Current-voltage characteristics of the diode with n-type Si/$B_{13}P_2$/n-type Si structure [73T].

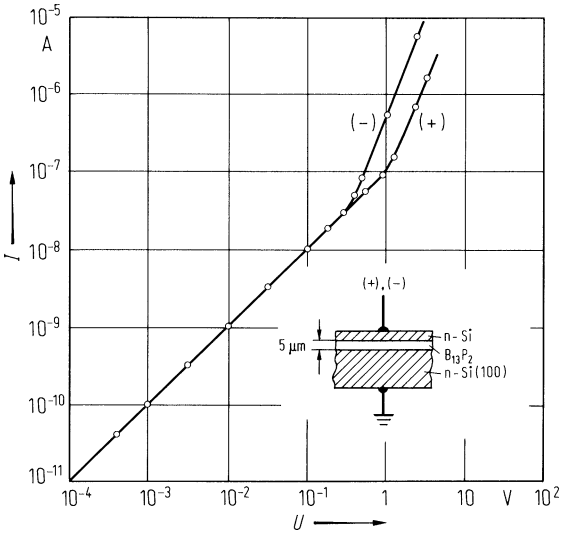

Fig. 9.

$B_{12}P_2$. Thermal conductivity of polycrystalline samples vs. temperature [71S]

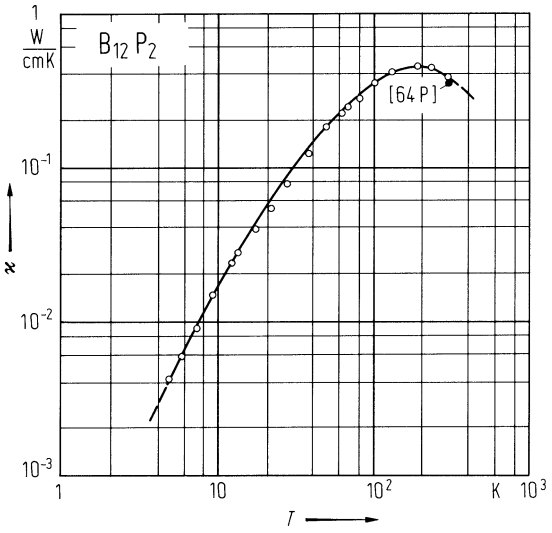

Fig. 10.

$B_{12}P_2$**.** Calculated optical properties. vs. photon energy. **(a)** Optical conductivity, **(b)** dielectric constants, **(c)** energy-loss function [95L]

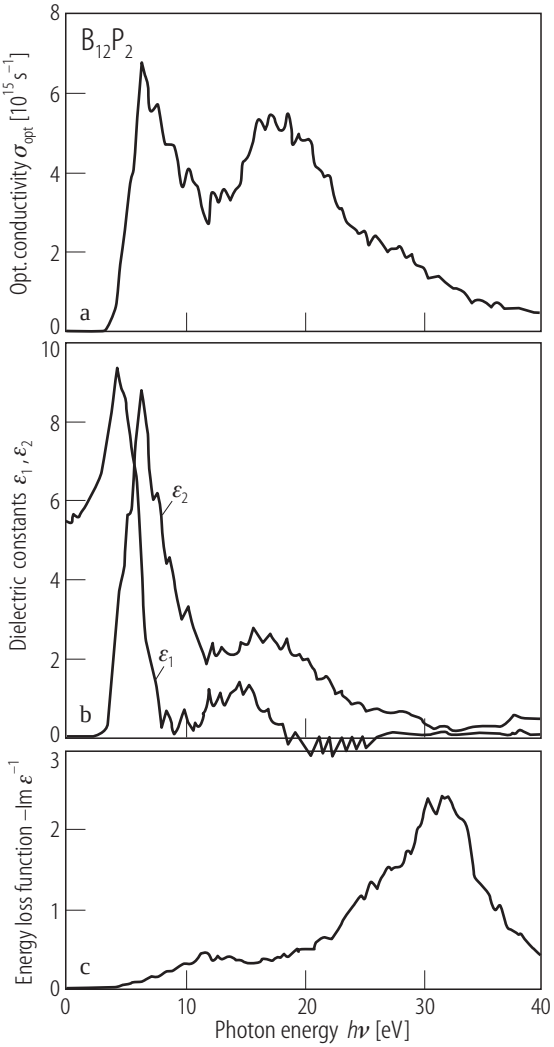

Fig. 11.

$B_{12}P_2$. Absorption edge of undoped [83S] and Si-doped $B_{12}P_2$ [96W, 97W]. Luminescence spectrum excited by an Nd:YAG laser [98S].

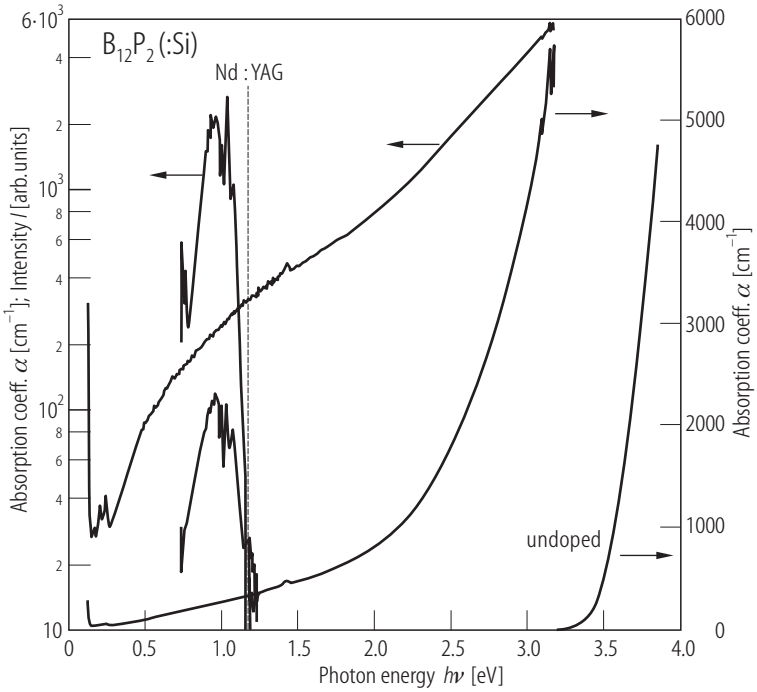

Fig. 12.

a-$B_{13}P_2$. Absorption edge; $(\alpha h\nu)^{1/3}$ vs. photon energy according to indirect forbidden interband transitions [91K, 95H].

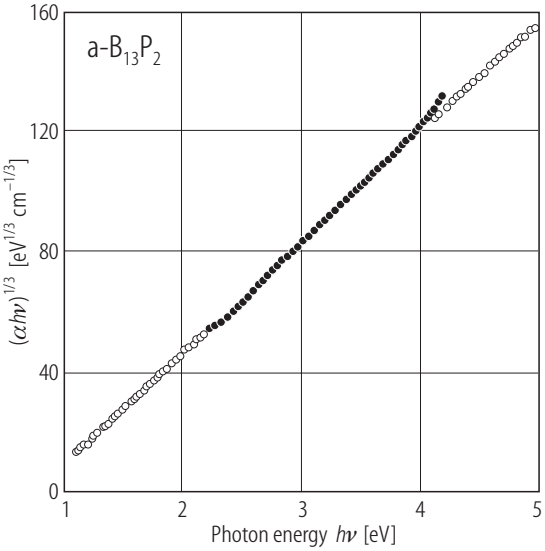

Fig. 13.

$B_{12}P_2$. One-phonon transmission and absorption spectra vs. wavenumber [97W]. In the center of the strongest peaks, the transmission is too low to determine the absorption coefficients reliably. At low wave numbers interferences within the 45 µm thick sample occur. The weak peaks in the ranges of low absorption (350...430 cm^{-1} and 650...730 cm^{-1}) are due to interferences as well. Because of the strong dispersion in these ranges, the evaluation is not meaningful.

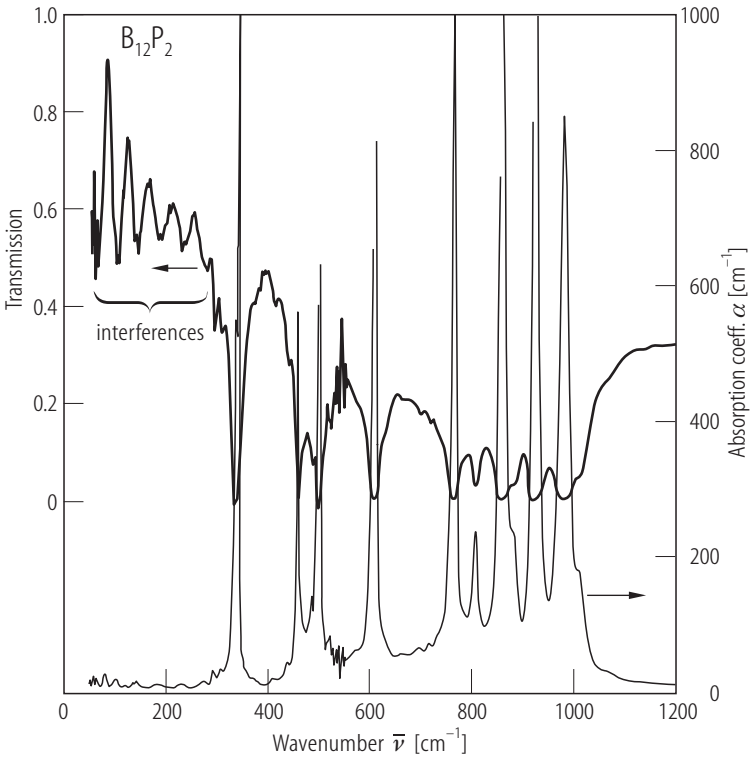

Fig. 14.

$B_{12}P_2$. Two-phonon spectrum of $B_{12}P_2$. vs. wavenumber [97W]. The weak equidistant peaks at the high-energy end of the spectrum are due to interferences.

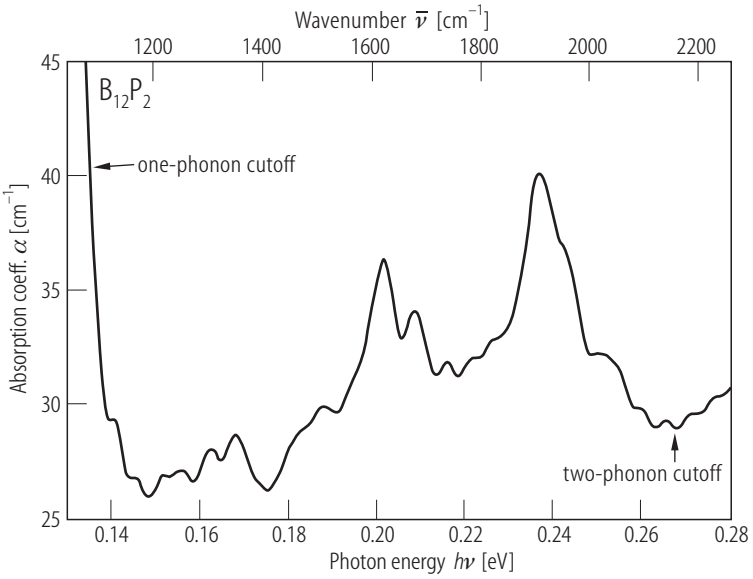

Fig. 15.

$B_{12}P_2$. Raman intensity vs. Raman shift; **(a)** conventionally measured spectra: Shirai [94S], Kumashiro [94K2], Aselage [97A]; **(b)** FT Raman spectra obtained with different equipments and intensities of the Nd:YAG lasers between 50mW and 4 W [96W, 97W, 99W].